Feasible Scaled Region of Teleoperation Based on the Unconditional Stability

Dal-Yeon Hwang, Blake Hannaford, and Hyoukryeol Choi

Abstract: Applications of scaled telemanipulation into micro or nano world that shows many different features from directly human interfaced tools have been increased continuously. Here, we have to consider many aspects of scaling such as force, position, and impedance. For instance, what will be the possible range of force and position scaling with a specific level of performance and stability? This knowledge of feasible scaling region can be critical to human operator safety. In this paper, we show the upper bound of the product of force and position scaling and simulation results of 1DOF scaled system by using the Llewellyn's unconditional stability in continuous and discrete domain showing the effect of sampling rate.

I. Introduction

Recent applications to the micro or nano world like micro-surgery which belongs to a macro-micro bilateral manipulation (MMBM) [5][10][11] shows the effectiveness of scaled teleoperation. Scaled teleoperation bridges the gap between H.O. (human operator) and task of object to be handled with the capability of scaling in factors such as force, position, impedance and power [3]. A teleoperation system is composed of several parts such as human operator, master robot or handle, communication channel, slave or remote robot and object. This multi parts involving makes the identification of the feasible operation region of scaled teleoperation very difficult due to accumulation of model error and time delay in and out of M and S. The operable region is limited by stability and performances [2][3][4][7]. Stability problem due to pure communication time delay between M (master) and S(slave) which is critical to space operation was solved in some aspect using lossless transmission line analogy [1]. Thereafter, this passivity approach has been popular to the researchers. However, this passivity-based control can lower performance down to 50% according to [4]. One of the reasons is due to low force reflection gain for the master. It is shown that position-error based force reflection combined with compliance control resulted in the best task performance when the set of normal master and big and stiff slave robot was used [9]. The overall system stability depends on the both of communication channel time delay, sampling rates and dynamics of M and S. To know the feasible operation region in terms of scaling factors such as position or force can be more helpful to a H.O. as MMBM spreads. So far, there have been few papers showing how feasible operation region depends on position and force scaling factors and sampling rates in nonidentical master and slave robots.

In this paper, we derived the upper bound of scaling gain product of position and force based on the unconditional stability. Then we identified the stable or feasible region of scaled teleoperation in terms of force, position scaling and sampling rates based on the characteristic equation when the time delay in each M, S are assumed to be from 0 to three sampling time (Ts). The communication channel delay is ignored. To include the time delay from sampling rates we used digital control model.

II. Two-port network and upper bound of scaling

1. Immittance of H matrix building

In this section we derive the upper bound of product of scalings, position and force based on two-port network passivity approach and Llewellyn's stability criteria [15]. The two-port network shape of a scaled teleoperation is shown in Fig.1. This features simplicity with no impedance shaping [12]. We added the force feedback line from the coordinated control input of the slave, g1 (Fig.1). We can refer more general control model from Lawrence (1993) which uses four channels of information for velocity and force. In scaled teleoperation, the master and slave are usually different in kinematic structure and dynamics, and control method for its own intended use. For the identification of scaling, we chose the unconditional stability criteria with the following reasons.

1) At the terminating points of M and H.O or S and environments, we can assume passive one-port terminations instead of two-port.

2) The Llewellyn's criteria which are less conservative for stability than the passivity condition [15] can provide a decoupled form for the scaling product.

$$\text{Re}(p_{11}) \geq 0, \qquad (1)$$

$$\text{Re}(p_{22}) \geq 0, \qquad (2)$$

$$2\,\text{Re}(p_{11})\text{Re}(p_{22}) \geq \left| p_{12}p_{21} \right| + \text{Re}(p_{12}p_{21}) \qquad (3)$$
$$, \forall \boldsymbol{w} \geq 0.$$

Define the matrix to be

$$P = \begin{bmatrix} p_{11} & p_{12} \\ p_{21} & p_{22} \end{bmatrix}$$

P is the immittance matrix of the two-port network system. P can be one of the matrixes such as the impedance Z, admittance Y or hybrid H. We chose the H matrix as the immi-

Dal-Yeon Hwang: Dept. of Mechanical Design Eng., Korea Polytechnic University(dyhwang@kpu.ac.kr)

Blake Hannaford: Dept. of Electrical Engineering, Univ. of Washington, USA(blake@u.washington.edu)

Hyoukryeol Choi: Dept. of Mechanical Engineering, Sungkyunkwan University(hrchoi@mecha.skku.ac.kr)

tance and derived the H parameters of Fig. 1 as follows before identifying the upper bound of scaling.

$$h_{11} = \frac{1}{G_m} + s_p s_f (g_1 G_c)(1 - \frac{G_c G_r}{G_c G_r + 1})$$

$$h_{12} = s_f (g_f + g_p \frac{G_c}{G_c + G_r^{-1}})$$

$$h_{21} = -s_p (\frac{G_c G_r}{G_c G_r + 1})$$

$$h_{22} = \frac{G_r}{1 + G_c G_r}$$

These h-parameters can have the other form according to the control architecture. However, we can observe that the scaling gains of s_p and s_f in h_{12}, h_{21} are in the product forms with the additional functions while these gains with extra functions are added to the master impedance.

$$P = \begin{bmatrix} \frac{1}{G_m} + s_p s_f g_1 G_c (1 - \frac{G_c G_r}{1 + G_c G_r}) & s_f (1 + g_1 \frac{G_c G_r}{1 + G_c G_r}) \\ -s_p \left(\frac{G_c G_r}{1 + G_c G_r} \right) & \frac{G_r}{1 + G_c G_r} \end{bmatrix}$$

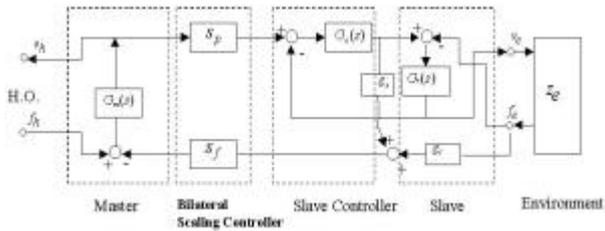$$= \begin{bmatrix} z_m + r_0 E & s_f F \\ -S_p D & J \end{bmatrix} \quad (4)$$

Fig. 1. Bilateral control of a scaled teleoperation in two-port network shape.

2. Upper bound of scaling by unconditional stability

If we apply Llewellyn's unconditional stability criteria, (3) into (4), we get the following condition.

$$\left((1 - \cos q)|FD| - 2 \cdot \mathrm{Re}(J)\mathrm{Re}(E) \right) \cdot r_0 \leq 2\mathrm{Re}(z_m)\mathrm{Re}(J)$$

If $(1 - \cos q)|FD| - 2\mathrm{Re}(J)\mathrm{Re}(E) > 0$ then

$$r_0 \leq V1 = \frac{2\mathrm{Re}(z_m)\mathrm{Re}(J)}{\left[(1 - \cos q)|FD| - 2\mathrm{Re}(J)\mathrm{Re}(E) \right]} \quad (5)$$

The product of position and force scaling, r_0 will have the upper bound as shown in (5),

Where $\qquad r_0 = s_p s_f$

$$D = \frac{G_c G_r}{1 + G_c G_r}$$

$$q = \angle(FD)$$

The other condition, (1) can impose a condition on the product of scalings, r0 since the p11 in (4) of which real part should not be negative. This leads to the following: From (1), (4)

$$\mathrm{Re}(\frac{1}{G_m} + r_0 E) \geq 0$$

If $\mathrm{Re}(E) > 0$, then $r_0 \geq -\dfrac{\mathrm{Re}(1/G_m)}{\mathrm{Re}(E)}$ (6a)

If $\mathrm{Re}(E) < 0$, then $r_0 \leq -\dfrac{\mathrm{Re}(1/G_m)}{\mathrm{Re}(E)}$ (6b)

This means that if the real part of E is positive, the product of scaling has a lower bound. Therefore, in our control architecture the product of scaling, r_0 is constrained by the conditions of (1) and (3). The H matrix as shown above is not reciprocal. Hence, there exists some difference between the passivity criteria and the unconditional stability [15].

In the simulation, we used a 1st order model for both of M and S with the slave force filter, $g_f = 0$ for simplicity. PI type global controller to velocity (see Fig. 2 caption) was used. We fixed all gains (ex, $s_f = 1$) except s_p during the simulation. The simulation result of upper bound of scaling is shown in Fig.2. Fig.2B shows three kinds of upper bounds for stable r_0 based on (a) LL's 1st condition, (b) LL's 3rd condition, (c) passivity condition. The upper bound of scaling based on LL's condition is about 8 (for w>=1.5 rad/sec) while the passivity condition presents the upper bound of 5.9. Here we should note that the scaling bound depends on the frequency. In this case, zero crossing point is shown at the frequency of 1.5 [rad/sec] below which r_0 has lower bound of a negative value. This can be explained by (6a), (6b), and Fig. 2C, 2D. Since we assumed r_0 to be positive for normal forward s_p and feedback s_f, any positive r_0 satisfies the (1).

In the following section we want to check the sampling rates and inherent time delay effects on the stability with position and force scaling by simulation. This analysis is based on the pole location criteria and the plant models of M, S that is from our former experimental set up [4][6]. Otherwise, we would face many troubles in setting the appropriate gains of controller and plants.

III. Scaling, sampling rates and stability based on characteristic equation

We used the following definition [15] to derive the stability criteria of the 2-port model of teleoperation.

Definition: A continuous (discrete) linear two-port network with given terminal immitances is stable if and only if the corresponding characteristic equation has no roots in the right half s-plane (outside the unit circle, z-plane) and only simple roots on the imaginary axis (unit circle).
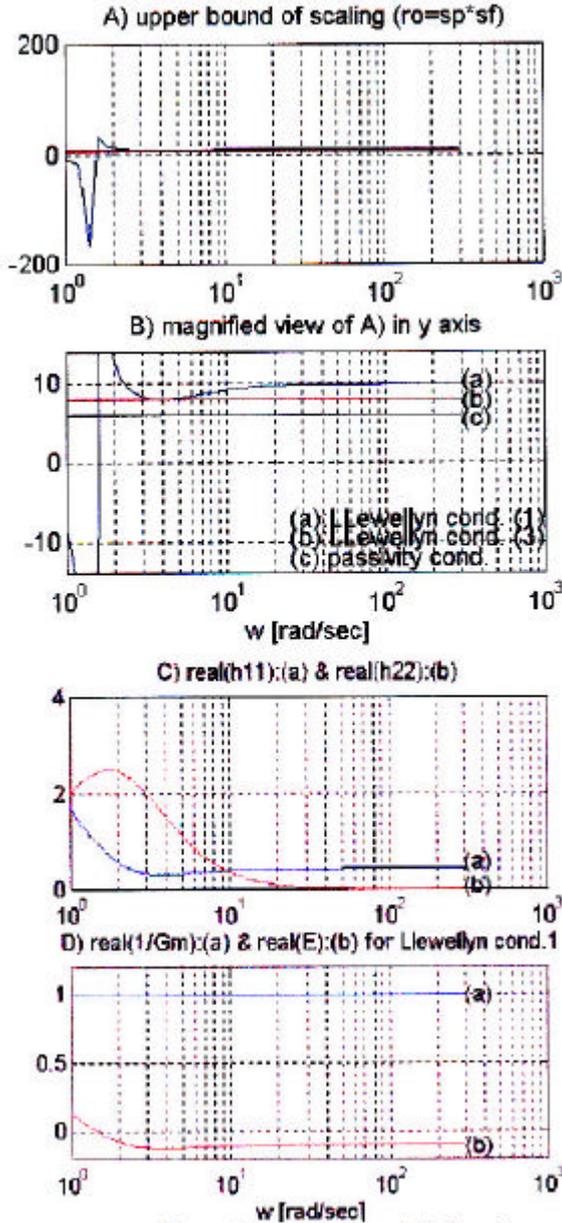
A) upper bound of scaling (ro=sp*sf)

B) magnified view of A) in y axis

(a): Llewellyn cond. (1)
(b): Llewellyn cond. (3)
(c): passivity cond.

w [rad/sec]

C) real(h11):(a) & real(h22):(b)

D) real(1/Gm):(a) & real(E):(b) for Llewellyn cond.1

w [rad/sec]

Fig. 2. Simulation of upper bound of scaling:
(a) Several scaling bounds, (b) Magnified view
of (a), (c) Real part of h11(s) and h22(s), (d)
Real part of 1/Gm(s) and E with sf=1, gp=1,
gf=0, Master plant (m=1, b= 1), Slave plant
(m=0.1, b=0.5), Gc=bc + kc/s (bc=-0.1, kc =0.3).

1. Transfer function of digital control

For simplicity, multiple of sampling time and same time delays in master and slave are assumed. H.O.'s force and environment external force are the inputs to the system while position or velocity of master and slave are the outputs. Forward flow (position/velocity) and backward effort (force) method is used (Hannaford, 1989). The control law used is a classical PD control for MS with coordinate torque.

$$S_p x_m - x_s = S_p v_m - v_s = 0 \qquad (7)$$

$$t_c = k_{c1}(x_m - x_s) + b_{c1}(v_m - v_s) \qquad (8)$$
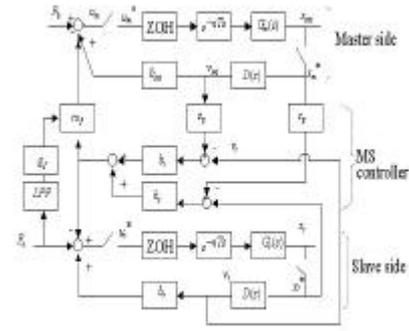

Fig. 3. Block diagram of 1DOF system for sampling rate
simulation, scaling and stability with ZOH.

We derive the transfer function from human operator force to slave position and master position in Z domain.
From Fig. 3,

$$X_r^* = G_{rp}^* U_r^* = G_{rp}^*(b_r D^* X_r^* + F_c^*) \qquad (9)$$

where X_r^* is the starred transform [14] and is defined as

$$X_r^* = X_r^*(s) = \sum_{n=0}^{\infty} X_r(nT) e^{-nTs}$$

The control input, coordinating torque for MS is

$$F_c^* = (k_c s_p + b_c s_p D^*) X_m^* - (k_c + b_c D^*) X_r^* \qquad (10)$$

The sampled master position is

$$\begin{aligned} X_m^* &= G_{mp}^* U_m^* \\ &= G_{mp}^*(F_h^* + b_m D^* X_m^* - rs_f F_c^*) \end{aligned} \qquad (11)$$

From (11)

$$X_m^* = \frac{G_{mp}^*(F_h^* - rs_f F_c^*)}{1 - G_{mp}^* b_m D^*} \qquad (12)$$

The coordinating torque is

$$F_c^* = h_1 X_m^* - h_2 X_r^* = h_2(s_p X_m^* - X_r^*) \qquad (13)$$

where
$$\begin{aligned} h_1 &= k_c s_p + b_c s_p D^* = s_p h_2 \\ h_2 &= k_c + b_c D^* \end{aligned}$$

Substituting (12) into (13)

$$\begin{aligned} F_c^* &= h_1\left(\frac{G_{mp}^*}{1 - G_{mp}^* b_m D^*} F_h^* - \frac{rs_f G_{mp}^*}{1 - G_{mp}^* b_m D^*} F_c^*\right) - h_2 X_r^* \\ &= h_1(h_3 F_h^* - h_4 F_c^*) - h_2 X_r^* \end{aligned} \qquad (14)$$

where

$$h_3 = \frac{G_{mp}^*}{1 - G_{mp}^* b_m D^*} \quad , \quad h_4 = \frac{rs_f G_{mp}^*}{1 - G_{mp}^* b_m D^*}$$

From (14),

$$F_c^* = g_1 F_h^* - g_2 X_r^* \qquad (15)$$

where $\qquad g_1 = \dfrac{h_1 h_3}{1 + h_1 h_4}, \qquad g_2 = \dfrac{h_2}{1 + h_1 h_4}$

Substituting (15) into (9)

$$X_r^* = G_{rp}^* b_r D^* X_r^* + G_{rp}^* \left(g_1 F_h^* - g_2 X_r^* \right) \qquad (16)$$

From (16)

$$T_{hr}^*(s) = \frac{X_r^*(s)}{F_h^*(s)} = \frac{g_1 G_{rp}^*}{1 + g_2 G_{rp}^* - b_r D^* G_{rp}^*} \qquad (17)$$

From (17), we can get the following expression

$$T_{hr}^*(s) = \frac{(s_p G_c) G_{mp}^* G_{rp}^*}{(L_m + s_p s_f r G_c G_{mp}^*) \cdot L_r - G_c\, G_{rp}^* L_m} \qquad (18)$$

where G_c : coordinated control for MS

$$G_c = k_c + b_c D^*$$

L_m : loop transfer function around master

$$L_m = 1 - b_m D^* G_{mp}^*$$

L_r : loop transfer function around slave

$$\underline{L_r = 1 - b_r D^* G_{rp}^*}$$

We can find $T_{hr}(z) = \dfrac{N_{hr}(z)}{D_{hr}(z)}$ from (17). From the denominator of (18), the product, r_0 (=sp*sf) is shown. We can plot root locus of the system about r_0.

2. Plant models for simulation

In this section the master and slave plant models in Z domain are introduced.

2.1 Master plant model

The master to be modeled is one DOF handle with the motion range of 180 degree, 150 mm long arm, driven by a brushed DC servo motor having 5.65 NM maximum torque [4][6]. The digital control model for the master shown in Fig. 3 is derived as

$G_{mp}(s) = zoh \cdot TimeDelay \cdot Plant$

$$= \frac{1 - e^{-Ts}}{s} \cdot e^{-sT_d} \frac{K_1 K_2}{s(J_m s + B_m)} \qquad (19)$$

where $J_m = 3.04$ [Nms^2/rad], $B_m = 0.156$ [Nms/rad]

The complete digital control model was built by Z-transform of (19).

2.2 Slave plant model

The slave plant to be modeled is a flat-coil magnetic head positioning actuator from a 1.8" hard disk drive of 1.18x 10^-3 Nm maximum torque which is 1/4790 of the master actuator. The slave has 40 degree motion range with a 30 mm long head arm. We used a 2nd order plant for the slave to reflect the spring effect from the printed circuit cable attached to the head arm.

$$G_{sp}(s) = \left(\frac{1 - e^{-Ts}}{s} \right) e^{-sTd} \left(\frac{k_3 k_4}{J_r s^2 + B_r s + K_r} \right) \qquad (20)$$

where $Jr = 2.39 x 10^{-7}$ [Nms^2/rad], $Br = 1.35 x 10^{-5}$ [Nms/rad], $K_r = 4.12 x 10^{-4}$ [Nm/rad]

2.3 Characteristic equation and its order

Characteristic equation, the denominator of (18) depends on the MS plants, global and local control, scaling gains of s$_p$, s$_f$, sampling rates and the assumed time delay.

In this work the communication time delay between the master and the slave was not considered because of the short distance. However, there is some time delay existing due to sampled control system causing some time duration between measuring data and output of actuator signal. This is believed to be 1 or 2 sampling time duration in a single system with some randomness. As the time delay increases by 1 Ts, the order of the global system increases by 2.

IV. Simulation

Stable scaling zone:

Table 1 shows the simulation cases varying sampling rate and assumed time delay. Time delays in each M and S are assumed from 0 to 3 Ts. Five cases of sampling rates from 1 KHz to 60 Hz are simulated.

Table 1. Case classification for simulation.

Fs Td	0 Ts	1 Ts	2 Ts	3 Ts
Sys.order	6	8	10	12
Case (a)	1 K Hz	1 K Hz	1 K Hz	1 K Hz
Case (b)	500 Hz	500	500	500
Case (c)	250 Hz	250	250	250
Case (d)	125 Hz	125	125	125
Case (e)	60 Hz	60	60	60

The simulation result with no time delay is shown in Fig. 4a-d where the horizontal plane is the operation region of position scaling, s$_p$ and force scaling, s$_f$ and Z axis is sampling time, Ts (1/sampling rate). Each curve in Fig. 4a is the boundary of stability. The upper right corner of the curve is unstable region while the lower left corner is stable one in the plane of Ts when s$_p$ is x-axis and s$_f$ is y-axis.
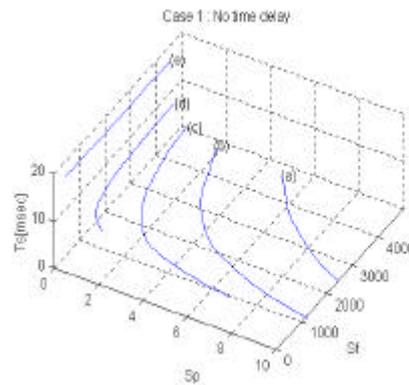

Fig. 4a. Stable scaling zone of position and force with no time delay showing wider feasible range.
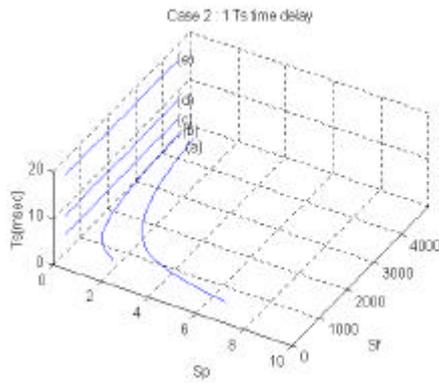
Fig. 4b. Stable scaling zone of position and force with 1 sampling time delay showing shrinkage of feasible domain.
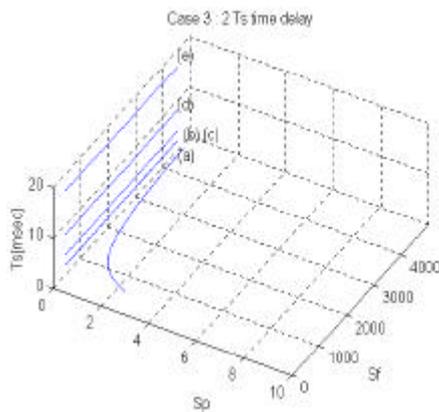

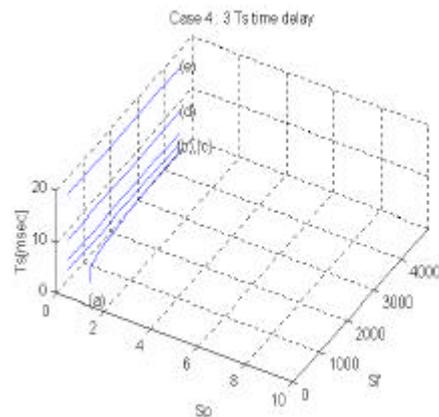Fig. 4c. Stable scaling zone of position and force with 2 sampling time delay.

Fig. 4d. Stable scaling zone of position and force with 3 sampling time delay.

VI. Conclusion

In section 2, we derived the upper bound of r0 (product of position and force scaling) using the Llewellyn's unconditional stability, which shows 25% larger value than passivity condition in a simple 1st order of master and slave. This confirms the less conservativeness of Llewellyn's condition in a non-reciprocal system. That the value of scaling product, r0 can be an index of the system stability is supported by [3][6], [18]. Daniel in [18] added two more indices of slave natural

frequency and mass ratio of master and slave in s domain. In the scaled teleoperation, the feasible region of scalings of position and force should be known for several reasons such as safety and full use of the system.

In the aspects of implementation, a teleoperation system is cascaded, multi-dynamics based and computer controlled. Hence, the sampling rates and the inherent time delay from the digital control system regardless of communication channel time delay deserves attention. We derived a transfer function that is from human operator to slave position in Z domain. We can summarize section 3, 4 simulation results as

The increase of one sampling time delay in both of master and slave leads to 2nd order addition to the system dynamics.

It should be noted that the rather big change of stable region of scaling factors, sp, sf depending on the randomness of time delay in computer controlled system can affect the operation and safety of teleoperation. The randomness should be studied further.

The stability based on the characteristic equation of Thr(z) is a SISO rather than MIMO. Hence, r0 from Thr(z) can be less conservative than r0 from passivity condition.

References

[1] R. J. Anderson and M. Spong, "Bilateral control of teleoperators with time delay," *Proc. IEEE Intl. Conf. Systems, Man & Cybernetics*, vol.1, pp.131-138, Beijing, China, Aug. 1988.

[2] G.J. Raju, G.C. Verghese, and B. Sheridan, "Design issue in two-port network models of bilateral remote teleoperation," *Proc. IEEE Intl. Conf. Robotics and Automation*, pp.1317-1321, 1989.

[3] B. Hannaford, "Design framework for teleoperators with kinesthetic feedback," *IEEE Transactions on Robotics and Automation*, vol. 5, no 4. Aug. 1989.

[4] C. A. Lawn and B. Hannaford, "Performance testing of passive communication and control in teleoperation with time delay," *IEEE Intern. Conf. on Robotics and Automation*, vol. 3, pp.776-781. Atlanta, GA, May,. 1993.

[5] H. Kobayashi and H. Nakamura, "A scaled teleoperation," *IEEE International Workshop on Robot and Human Communication*, pp.269-274, 1992.

[6] D. Y. Hwang and B. Hannaford, "Modeling and stability analysis of a scaled telemanipulation system," *IEEE International Workshop on Robot and Human Communication*, pp.32-37, 1994.

[7] D.Y. Hwang and B. Hannaford, "Teleoperation performance with kinematically redundant slave robot," *International Journal of Robotics Research*, vol 17, no.6, pp.579-597, June 1998.

[8] B. H. Choi, W. J. Jung, and H. K Choi, "Study for control of Master-Slave teleoperation system with time delay," KSME, vol23 A, pp.57-65, 1999.

[9] W. S. Kim, "Developments of new force reflecting control schemes and an application to a teleoperation training simulator," *IEEE Intern. Conf. on Robotics and Automation*, pp. 1412-1419, Nice, France, May 1992.

[10] T. Fukuda, T., K. Tanie, and T. Mitusuoka, "A new method of master-slave type of teleoperation for a micro-

manipulator system," *IEEE Micro Robots and Teleopera-tors Workshop, Hyannis, Massachusetts*, Nov. 1987.

[11] J. E. Colgate, "Power and impedance scaling in bilateral manipulation," *IEEE Intern. Conf. on Robotics and Automation, Sacramento, California*, April 1991.

[12] J. E. Colgate, "Coupled stability of multiport systems - theory and experiments," *Trans. ASME, Journal of Dynamic Systems, Measurement, and Control*, vol. 116, no.3, pp.419-28, 1994.

[13] Y. Yokokohji, N. Hosotani and, T. Yoshikawa, "Analysis of maneuverability and stability of micro-teleoperation systems," *IEEE Conf. R&A*, 1994.

[14] C. L Phillips, H.T. Nagle, Jr., 1984, *Digital Control System Analysis and Design*, Prentice-Hall. Englewood Cliffs, N.J.

[15] R. J. Adams, B. Hannaford, "Stable haptic interaction with virtual environments," *IEEE Transactions on Robotics and Automation*, vol. 15, no. 3, 1999, pp.465-474.

[16] D. A. Lawrence, "Stability and transparency in bilateral teleoperation," *IEEE Transactions on Robotics and Automation*, vol. 9, no.5, October, 1993.

[17] Y. Strassberg, "A control method for bilateral teleoperating systems," Ph.D. Thesis, Dept. of Mech., Univ. of Toronto, 1992.

[18] R. W. Daniel and P. R. McAree, "Fundamental limits of performance for force reflecting teleoperation," *Int. J. of Robotics Research*, vol. 17, no.8, pp.811-830, Aug. 1998.

[19] K. Hashhadt, "A control method for bilateral teleoperating systems," Ph.D. Thesis, Dept. of EE & CSE., Univ. of British Columbia, 2000.

Dal-Yeon Hwang
He received B.S degree from Seoul National University in 1983 and M.S degree in mechanical engineering from KAIST in 1985,and Ph.D. degree in electrical engineering, University of Washington in 1995, USA. Now, he is an Assistant Professor in Dept. of Mechanical Design Engineering, Korea Polytechnic University, Korea. He worked as a principal researcher in Production Engineering Resh. center of LG electronics from 1985 to 1999. His interests include teleoperation and haptics, field applications of robot and machine vision, microelectronics packaging.

Blake Hannaford
He received the B.S. deg. in Engineering and Applied Science from Yale University in 1977, and the M.S. and Ph.D. degrees in Electrical Eng. from the University of California, Berkeley, in1982 and 1985 respectively. From 1986 to 1989 he worked on the remote control of robot manipulators in the Man-Machine Systems Group in the Automated Systems Section of the NASA Jet Propulsion Laboratory, Caltech. He supervised that group from 1988 to 1989. Since September 1989, he has been at the University of Washington in Seattle, where he has been Professor of Electrical Engineering since 1997, and served as Associate Chair for Education from 1999 to 2001. He was awarded the National Science Foundation's Presidential Young Investigator Award and the Early Career Achievement Award from the IEEE Engineering in Medicine and Biology Society. His currently active interests include haptic displays on the internet, and surgical biomechanics. He is the founding editor of Haptics-e, The Electronic Journal of Haptics Research(www.haptics-e.org). His lab URL is http://rcs.ee.washington.edu/BRL.

Hyoukryeol Choi
He received B.S degree from Seoul National University in 1984, M.S degree from KAIST in 1986, and Ph.D. degree from Pohang University of Science and Technology in 1994, Korea. Now, he is an Associate Professor in School of Mechanical Engineering, Sungkyunkwan University. He worked as an associate researcher in LG electronics from 1986 to 1989.

From 1993 to 1995 he stayed in Kyoto University, and from 2000 to 2001 in Advanced Institute of Industrial Science and Technology (AIST), Japan as an invited researcher.

His interests include dextrous mechanisms, field applications of robotics, micro actuators and micro robots.